Title	Time-varying correlation coefficients estimation and its application to dynamic connectivity analysis of fMRI
Author(s)	Fu, Z; Di, X; Chan, SC; Hung, YS; Biswal, BB; Zhang, Z
Citation	The 35th Annual International Conference of the IEEE Engineering in Medicine and Biology Society (EMBC 2013), Osaka, Japan, 3-7 July 2013. In IEEE Engineering in Medicine and Biology Society Conference Proceedings, 2013, p. 2944-2947
Issued Date	2013
URL	http://hdl.handle.net/10722/189877
Rights	IEEE Engineering in Medicine and Biology Society. Conference Proceedings. Copyright © IEEE.

35th Annual International Conference of the IEEE EMBS
Osaka, Japan, 3 - 7 July, 2013

Time-varying Correlation Coefficients Estimation and its Application to Dynamic Connectivity Analysis of fMRI

Zening Fu[1], Xin Di[2], Shing-Chow Chan[1], Yeung-Sam Hung[1], Bharat B. Biswal[2] and Zhiguo Zhang[1]

Abstract— **Exploration of the dynamics of functional brain connectivity based on the correlation coefficients of functional magnetic resonance imaging (fMRI) data is important for understanding the brain mechanisms. Because fMRI data are time-varying in nature, the functional connectivity shows substantial fluctuations and dynamic characteristics. However, an effective method for estimating time-varying functional connectivity is lacking, which is mainly due to the difficulty in choosing an appropriate window to localize the time-varying correlation coefficients (TVCC). This paper introduces a novel method for adaptively estimating the TVCC of non-stationary signals and studies its application to infer dynamic functional connectivity of fMRI data in a visual task. The proposed method employs a sliding window having a certain bandwidth to estimate the TVCC locally and the window bandwidths are selected adaptively by a local plug-in rule to minimize the mean squared error. The results show that the functional connectivity changes in the visual task are transient, which suggests that simply assuming sustained connectivity changes during task period might not be sufficient to capture dynamic connectivity changes induced by tasks.**

I. Introduction

Recent years have witnessed a significant shift in human brain function research from functional segregation (i.e., to localize activated brain regions associated with specific functions) towards functional integration (i.e., to explore connectivity among brain regions for specific functions). The study of functional brain connectivity (especially, the task modulated connectivity changes) from functional magnetic resonance imaging (fMRI) data has been drawing increasing interests because it is able to reveal the statistical dependence among distributed brain regions with high spatial resolution. However, the conventional functional connectivity analysis approaches are usually model-based and implicitly assume sustained changes of connectivity during the whole task condition, e.g. psycho-physiological interaction (PPI) [1] and dynamic causal modeling (DCM) [2]. Hence, a data-driven method, which does not assume any prior structural or biophysical knowledge, is needed to justify whether connectivity changes in the task are sustained over time.

In statistics, the Pearson product-moment correlation coefficient is a measure of connectivity between two variables [3, 4] and it is also a fundamental tool for inferring functional connectivity among distributed cortical regions from fMRI data. For stationary signals, the correlation coefficient is independent of time. However, fMRI data are non-stationary in nature and carry meaningful information that fluctuates with time. As a result, the correlation coefficients among fMRI time courses are time-varying as well. Most studies on functional connectivity only assume the correlation coefficients are fixed [5, 6] so that the important dynamic changes of the connectivity are totally overlooked. A simple but effective time-varying correlation coefficient (TVCC) estimation approach is to use a sliding window, which assigns larger weights to neighboring data and smaller weights to remote data, to localize the correlation information [7]. The selection of the window size is extremely critical to the TVCC estimation approach. For slow varying covariance, a large window size is desirable so that more accurate estimates can be obtained by averaging out the additive noise. In contrast, a small window is preferred for estimating fast varying covariance. Generally, a window with a suitable size could help avoid the excessive bias and reduce the estimation variance [8]. However, how to select an appropriate window for TVCC estimation is still an open problem.

In this paper, we adopt a local plug-in rule [9, 10] to adaptively select the window bandwidth in TVCC estimation to address the bias-variance tradeoff problem mentioned above. The basic idea of the plug-in rule is that the optimal local bandwidth should minimize the mean integrated squared error (MISE) of windowed covariance. Compared with conventional sliding-window based approaches, the novel adaptive windowed TVCC (AW-TVCC) estimation method is capable of selecting window size adaptively so as to avoid possible over- or under-smoothing due to inappropriate window selection. Simulation results show that the proposed method can achieve better accuracy than TVCC estimation with a fixed window size. Further, we apply the proposed AW-TVCC method to identify time-varying functional connectivity of fMRI in a visual task. Experiment results show that the connectivity changes during viewing checkerboard were not fixed but showed considerably transient patterns. Thus simply assuming sustained connectivity changes during task period might not be sufficient to capture the dynamic connectivity information.

The rest of this paper is organized as follows. The AW-TVCC estimation and its adaptive bandwidth selection method using the local plug-in rule are introduced in Section II. In Section III, we test the performance of the AW-TVCC estimator using simulated signals and then apply it in visual task based fMRI dataset to analyze the transient changes of

*Research supported by a GRF grant from the Research Grants Council of the Hong Kong SAR (HKU 767511M) and a HKU CRCG Seed Funding for Basic Research (201203159009).

Zening Fu, Shing-Chow Chan, Yeung-Sam Hung and Zhiguo Zhang are with the Department of Electrical and Electronic Engineering, The University of Hong Kong, China (e-mail: zgzhang@eee.hku.hk).

Xin Di and Bharat B. Biswal are with the Department of Biomedical Engineering, New Jersey Institute of Technology, Newark, NJ, USA.

connectivity between different brain regions. Finally, conclusion is drawn in Section IV.

II. Adaptive Windowed TVCC Estimation

A. TVCC Matrix

Given a group of discrete-time random processes $\mathbf{x}(n) = [\boldsymbol{x}_1(n), \cdots, \boldsymbol{x}_k(n)]$, $n = 1,2,\cdots,N$, k is the number of the processes and N is the number of time samples. The estimate of the $k \times k$ covariance matrix is:

$$\mathbf{Cov} = \frac{1}{N}\sum_{n=1}^{N}\begin{bmatrix} \boldsymbol{x}_1(n)\boldsymbol{x}_1(n) & \cdots & \boldsymbol{x}_k(n)\boldsymbol{x}_1(n) \\ \vdots & \ddots & \vdots \\ \boldsymbol{x}_k(n)\boldsymbol{x}_1(n) & \cdots & \boldsymbol{x}_k(n)\boldsymbol{x}_k(n) \end{bmatrix}. \quad (1)$$

Hence, the correlation coefficient matrix is given by:

$$\mathbf{CC} = \begin{bmatrix} \frac{\mathbf{Cov}_{11}}{\sqrt{\mathbf{Cov}_{11}\mathbf{Cov}_{11}}} & \cdots & \frac{\mathbf{Cov}_{1k}}{\sqrt{\mathbf{Cov}_{11}\mathbf{Cov}_{kk}}} \\ \vdots & \ddots & \vdots \\ \frac{\mathbf{Cov}_{1k}}{\sqrt{\mathbf{Cov}_{11}\mathbf{Cov}_{kk}}} & \cdots & \frac{\mathbf{Cov}_{kk}}{\sqrt{\mathbf{Cov}_{kk}\mathbf{Cov}_{kk}}} \end{bmatrix}, \quad (2)$$

where $\mathbf{Cov}_{i,j}$ is the observed (i,j)-th entry of **Cov** matrix.

For non-stationary signals, the time-varying covariance (TVCOV) matrix at each time instant n is:

$$\mathbf{Cov}(n) = E[\mathbf{x}(n)\mathbf{x}^H(n)], \quad (3)$$

where $\mathbf{x}^H$ is the inverse of $\mathbf{x}$.

Since the prior information of $\mathbf{x}(n)$ is unknown, it is difficult to calculate the TVCOV analytically. In local estimation, TVCOV can be estimated by using the sliding-window approach. More precisely, $\mathbf{Cov}(n)$ can be calculated from the local data segment, which is assumed to be stationary, using a sliding window that assigns large weights on local samples and small weights on remote samples. The window is generally selected as a positive value function over time with finite second moment and symmetric around the origin. The corresponding TVCOV can be expressed as:

$$\mathbf{Cov}(n;h) = \sum_{m=-h}^{h} K_h(m)\mathbf{x}(n+m)\mathbf{x}^H(n+m), \quad (4)$$

where $K_h(u) = \frac{1}{h}K(u/h)$ is the kernel controlled by a bandwidth h. The selection of the bandwidth is critical to the accuracy of the estimation and thus adaptive bandwidths are desired [11].

Therefore, the TVCC can be computed from the TVCOV as:

$$\mathbf{CC}(n) = \begin{bmatrix} \frac{\mathbf{Cov}_{11}(n)}{\sqrt{\mathbf{Cov}_{11}(n)\mathbf{Cov}_{11}(n)}} & \cdots & \frac{\mathbf{Cov}_{1k}(n)}{\sqrt{\mathbf{Cov}_{11}(n)\mathbf{Cov}_{kk}(n)}} \\ \vdots & \ddots & \vdots \\ \frac{\mathbf{Cov}_{1k}(n)}{\sqrt{\mathbf{Cov}_{11}(n)\mathbf{Cov}_{kk}(n)}} & \cdots & \frac{\mathbf{Cov}_{kk}}{\sqrt{\mathbf{Cov}_{kk}(n)\mathbf{Cov}_{kk}(n)}} \end{bmatrix}. \quad (5)$$

B. Adaptive Window Selection

Considering each entry of the matrix $\mathbf{x}(n)\mathbf{x}^H(n)$ as a non-stationary process:

$$\boldsymbol{X}_{i,j}(n) = \boldsymbol{r}_{i,j}(n) + \varepsilon_n, \quad i,j = 1,2,\cdots,k, \quad (6)$$

where $\boldsymbol{X}_{i,j}(n) = \boldsymbol{x}_i(n)\boldsymbol{x}_j(n)$ is the observed (i,j)-th entry of $\mathbf{x}(n)\mathbf{x}^H(n)$. The regression function $\boldsymbol{r}(n)$ is four times continuously differentiable and ε is a zero mean Gaussian process with variance σ^2. By employing local estimation [9] on the data, the estimator $\hat{\boldsymbol{r}}(n)$ for the regression curve can be written as:

$$\mathbf{Cov}_{i,j}(n,h(n)) = \hat{\boldsymbol{r}}(n,h(n)) = \frac{1}{h(n)}\sum_{s=1}^{N} K\left(\frac{s-n}{h(n)}\right)\boldsymbol{X}_{i,j}(s), \quad (7)$$

where $h(n)$ is the selected local bandwidth.

The mean squared error (MSE) $\mathrm{MSE}(\boldsymbol{r}(n;h(n))) = E(\hat{\boldsymbol{r}}(n;h(n)) - \boldsymbol{r}(n))^2$ provides a local measure for the quality of the performance of the estimator. To decrease the influence of boundary effects, a weight function $\boldsymbol{v}$ is used in the MISE which characterizes the global behavior of the estimator. Hence, a global plug-in bandwidth estimator should minimize the MISE and asymptotically optimal bandwidth is given by:

$$h_{ASY} = \left(\frac{\sigma^2\psi\sum_{s=1}^{N}\boldsymbol{v}(s)}{N\mu_2^2\sum_{s=1}^{N}\boldsymbol{v}(s)\boldsymbol{r}''(s)^2}\right)^{1/5}, \quad (8)$$

where $\psi = \int K^2(x)dx$ and $\mu_2 = \int K(x)x^2dx > 0$ are kernel parameters, s is the time instant.

As the asymptotically optimal bandwidth above cannot be computed directly, an iterative algorithm is proposed in [9,12,13] and some modifications have been made for obtaining a local bandwidth estimator for TVCOV. The details of the algorithm are given in TABLE I.

TABLE I. Local Plug-in Estimator for TVCOV

At each time instant n
Step 1. Set an initial bandwidth $\hat{h}_0(n) = N^{-1}$.
Step 2. Iterate $\hat{h}_i(n) = \left(\frac{\hat{\sigma}^2\psi\sum_{s=1}^{N}\boldsymbol{v}(s)}{N\mu_2^2\sum_{s=1}^{N}\boldsymbol{v}(s)\hat{\boldsymbol{r}}''(s;\hat{h}_{i-1}(n)N^{1/10})}\right)^{1/5}$, for $i = 1,\cdots,8$.
Step 3. Iterate $\hat{h}_i(n) = \left(\frac{\hat{\sigma}^2\psi\sum_{s=1}^{N}\boldsymbol{v}(s)}{N\mu_2^2\sum_{s=1}^{N}K\left(\frac{s-n}{\hat{h}_{i-1}(n)}\right)\hat{\boldsymbol{r}}''(s;\hat{h}_{i-1}(n)N^{1/10})}\right)^{1/5}$, for $i = 9,10$.
Step 4. Let $\hat{h}_{10}(n)$ be the optimal bandwidth at n.

The first eight iteration steps are necessary to stabilize the estimator and yield the correct rate of $N^{1/5}$ [9]. In TABLE I. σ^2 can be estimated as:

$$\hat{\sigma}^2 = \frac{1}{2(N-1)}\sum_{n=1}^{N-1}(\boldsymbol{X}_{i,j}(n+1) - \boldsymbol{X}_{i,j}(n))^2. \quad (9)$$

The second derivative of $\hat{\boldsymbol{r}}$ is estimated by a kernel estimator with the bandwidth $\tilde{h}$:

$$\hat{\boldsymbol{r}}''(n;\tilde{h}) = \frac{1}{N\tilde{h}^3}\sum_{s=1}^{N}\tilde{K}\left(\frac{s-n}{\tilde{h}}\right)\boldsymbol{X}_{i,j}(s), \qquad (10)$$

where $\tilde{K}$ is a kernel satisfying the condition in [9] and $\tilde{h} = h_i(n)N^{1/10}$, where $N^{1/10}$ is the inflation factor which leads to a bandwidth selector with a variance of the smallest possible order.

The above algorithm can estimate the local adaptive bandwidth of each entry to calculate the TVCOV matrix. Then we need to compute the TVCC matrix from TVCOV matrix. However, as different entries of the TVCOV are independently estimated with different bandwidths, the TVCC matrix estimated may not be positive definite. To solve this problem, a universal bandwidth for all entries of the TVCOV is needed at each time instant. Here, we propose to approximate the universal bandwidth as the average of the optimal local bandwidths of all entries of the TVCOV, and such approximation works well in the experiments.

III. Experiments and Results

A. Simulation Test

In this simulation, two discrete-time signals $\boldsymbol{x}_1(n), \boldsymbol{x}_2(n)$ were used to evaluate the performance of the proposed and conventional methods. $\boldsymbol{x}_1(n)$ was chosen as $\boldsymbol{x}_1(n) = \sin(\frac{\pi}{100}n) + \sin(\frac{\pi}{50}n)$, $1 \le n \le 1200$ and $\boldsymbol{x}_2(n)$ was chosen as:

$$\begin{cases} \boldsymbol{x}_2(n) = -\boldsymbol{x}_1(n), & 1 \le n \le 200, 401 \le n \le 600, 801 \le n \le 1000, \\ \boldsymbol{x}_2(n) = \boldsymbol{x}_1(n), & 201 < n \le 400, 601 \le n \le 800, 1001 \le n \le 1200. \end{cases}$$

Hence, the correlation coefficients of these two signals are time-varying as:

$$\mathbf{CC}_{12}(n) = \begin{cases} -1 & 1 \le n \le 200, 401 \le n \le 600, 801 \le n \le 1000, \\ 1 & 201 < n \le 400, 601 \le n \le 800, 1001 \le n \le 1200. \end{cases}$$

The Epanechnikov kernel $K(h) = \frac{3}{4}(1-h^2)$ was chosen as the kernel function in the AW-TVCC method.

We compared the AW-TVCC method and the conventional method with different fixed bandwidths (4, 20, 40 and 60) quantitatively by computing the MSE of the TVCC estimation under Gaussian noises with different SNRs (20dB and 30dB). TABLE II. is obtained from averages of 50 independent simulations. It can be seen that the MSE of the AW-TVCC method is smaller than MSEs of the method with fixed bandwidths, which proves that the proposed AW-TVCC method can achieve more accurate estimation of TVCCs than conventional estimator with fixed bandwidths.

TABLE II. MSEs of Different Methods

	$h=4$	$h=20$	$h=40$	$h=60$	Adaptive bandwidth
SNR = 10	0.0075	0.0118	0.0254	0.0473	0.0043
SNR = 20	0.0492	0.0196	0.0304	0.0511	0.0184

B. Analysis of the TVCCs of fMRI dataset

We further studied visually induced connectivity changes when subjects were viewing checkerboard flickering. The fMRI data were collected from fourteen male subjects aged from 16 to 60 years (mean: 40.2 years). All participants were given written informed consent and the local ethics committee approved the experimental procedures. The fMRI data have 240 images and were derived from the NKI-RS multiband imaging Test-Retest Pilot Dataset. The fMRI scan comprised of 20s fixation, 20s flickering checkerboard viewing, with a repetition of three times followed by a fixation condition at the end of the scan. The TR is 0.645 second and the voxel size is 3 mm^3 isotropic.

Firstly, the preprocessing of the fMRI was performed using SPM8 (http://www.fil.ion.ucl.ac.uk/spm/), including motion correction, normalization of the functional images via normalizing the anatomical image and spatial smoothing using an 8mm Gaussian kernel. Moreover, we used general linear model (GLM) to get activation relating to the checkerboard condition. According to the activation maps, four regions of interest (ROIs) were defined in Figure 1. : right middle occipital gyrus (MOG), left MOG, right fusiform gyrus (FuG), and left FuG. The time series from the four ROIs were extracted after removing head motion parameters and signals from the white matter and cerebrospinal fluid.

Secondly, the proposed novel AW-TVCC estimation method was used to investigate the changes of the connectivity between each pair of the ROIs. To evaluate the task related changes of the connectivity, for each post-stimulus time point (0~30s), its p-value was computed by locating the fMRI or TVCC value under the probability density function approximated from the population of pre-stimulus samples (-10~0s).

Figure 2. shows that the fMRI time-courses and their TVCCs have clear three-cycle periodical patterns. The spectral analysis of fMRI time-courses and their TVCCs were displayed in Figure 3. which shows that the TVCCs have a main frequency component around 0.025Hz. Moreover, the TVCCs also exhibit higher frequency components (around 0.045Hz), indicating more complex pattern of connectivity changes.

Figure 4. shows the statistic results of the fMRI time-courses and TVCCs. The TVCCs in the post-stimulus period, especially the TVCCs between (i) LMOG and LFuG, and (ii) RMOG and RFuG, increase immediately and faster than the increases of fMRI time-courses. However, compared with the sustained responses of BOLD activities, the TVCCs decrease below the pre-stimulus baseline at the end of the task.

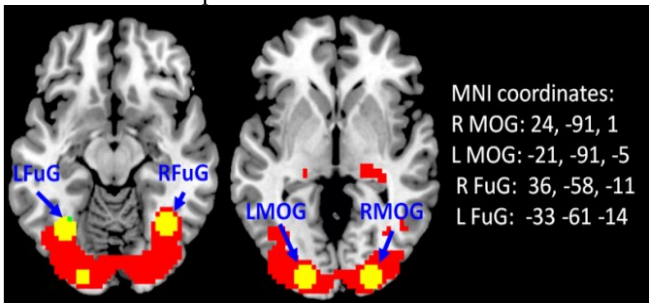

Figure 1. The group activation map for the checkerboard stimuli. Four Yellow circles indicated the ROIs

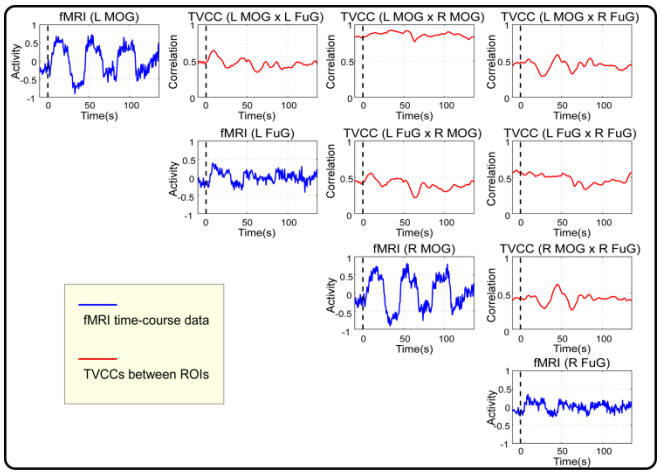

Figure 2. fMRI time-courses of 4 ROIs and their TVCC estimates (averaged across 14 subjects).

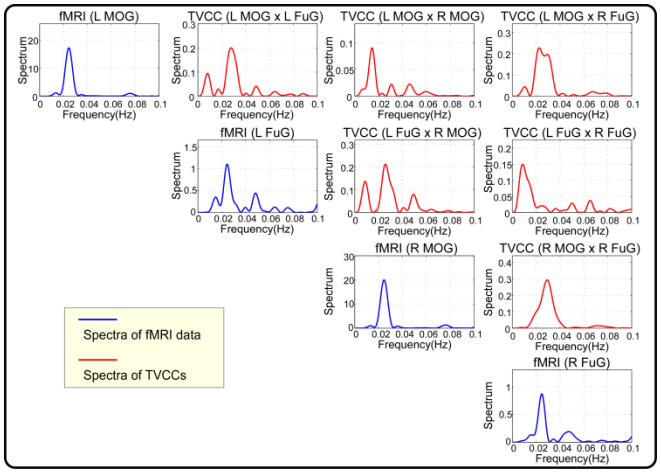

Figure 3. Spectra of fMRI time-courses and their TVCC estimates (averaged across 14 subjects).

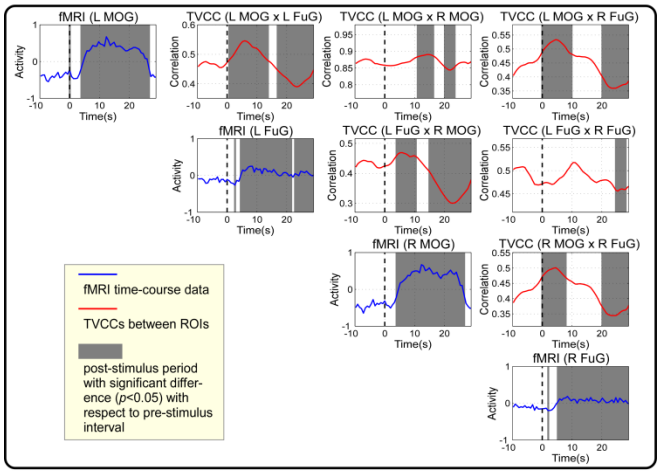

Figure 4. The statistical analysis is performed on fMRI time-courses and TVCCs to show the significant difference (shadow region) between the data within the post-stimulus interval and those within the pre-stimulus interval. The fMRI time-courses and TVCCs are averaged across three cycles and fourteen subjects and segmented into pre-stimulus interval (-10s to 0 s) and post-stimulus interval (0 s to 30 s).

IV. Conclusion

A new AW-TVCC estimator is presented in this paper. The AW-TVCC method is based on local estimation and employs a sliding window with adaptively-selected local bandwidths to address the bias-variance tradeoff problem encountered in TVCC estimation. The proposed adaptive method has been demonstrated to provide an accurate estimation of dynamic connectivity among fMRI time-series. In conventional fMRI studies, the functional connectivity patterns are usually assumed to be static. However, our results revealed that the functional connectivity in a visual task is significantly dynamic. The dynamic functional connectivity may covey important information about the underlying physiological and psychological states of subjects, and the relationship between such dynamic functional connectivity and behavior or physiological parameters will be left for future study.

References

[1] K. J. Friston, C. Buechel, G. R. Fink, J. Morris, E. Rolls, and R. J. Dolan, "Psychophysiological and modulatory interactions in neuroimaging," *Neuroimage*, vol. 6, no. 3, pp. 219-228, 1997.

[2] K. J. Friston, L. Harrison, and W. Penny, "Dynamic causal modelling," *Neuroimage*, vol. 19, no. 4, pp. 1273-1302, 2003.

[3] J. L. Rodgers and W. A. Nicewander, "Thirteen ways to look at the correlation coefficient," *The American Statistician*, vol. 42, no. 1, pp. 59-66, 1988.

[4] S. M. Stigler, "Francis Galton's Account of the Invention of Correlation," *Stat. Sci.*, vol. 4, no. 2, pp. 73-79, 1989.

[5] T. Koenig, D. Studer, D. Hubl, L. Melie, and W. K. Strik, "Brain connectivity at different time-scales measured with EEG," *Philos. Trans. R. Soc. Lond. B Biol. Sci.,* vol. 360, no. 1457, pp. 1015-1023, 2005.

[6] L. Hu, and Z. G. Zhang, and Y. Hu, "A time-varying source connectivity approach to reveal human somatosensory information processing," *Neuroimage,* 2012.

[7] M. Ozgen, "Extension of the capon's spectral estimator to time–frequency analysis and to the analysis of polynomial-phase signals," *Signal Process.*, vol. 83, no. 3, pp. 575–592, 2003.

[8] Z. G. Zhang, S. C. Chan, K. H. Ho, and K. C. Ho, "On bandwidth selection in local polynomial regression analysis and its application to multi-resolution analysis of non-uniform data," *J. Signal Process. Syst.*, vol. 52, no. 3, pp. 263–280, Sep.2008.

[9] M. Brockmann, T. Gasser, and E. Herrmann, "Locally adaptive bandwidth choice for kernel regression estimators," *J. Am. Stat. Assoc.*, vol. 88, no. 424, pp. 1302–1309, 1993.

[10] E. Herrmann, "Local bandwidth choice in kernel regression estimation," *J. Comput. Graph. Stat.,* vol. 6, no. 1, pp. 35-54, 1997.

[11] G. Motta, C. Hafner, and R. von Sachs, "Locally stationary factor models: Identification and nonparametric estimation," *Economet. Theory*, vol. 27, no. 6, p. 1279, 2011.

[12] T. Gasser, L. Sroka, and C. Jennen-Steinmetz, "Residual variance and residual pattern in nonlinear regression," *Biometrika*, vol. 73, no. 3, pp. 625–633, 1986.

[13] T. Gasser and H. G. Muller, "Estimating regression functions and their derivatives by the kernel method," *Scand. J. Stat.*, vol.11, pp.171-185, 1984.